IMAGE SEGMENTATION FOR INDUSTRIAL QUALITY INSPECTION

Dr. Catalin Gh**. AMZA**, Universitatea Politehnica din Bucuresti, acata1@camis.pub.ro
Dr. Gheorghe **AMZA,** Universitatea Politehnica din Bucuresti, amza@camis.pub.ro
Dr. Diana **POPESCU,** Universitatea Politehnica din Bucuresti, dian_popescu@yahoo.com

Abstract*: The contaminant detection process of an industrial product is an important stage of a modern production factory. The large demand of quality products has lead producers to use automated systems. One such system is the automated detection of defects/contaminants. An X-ray image of the product is taken and automatically analysed by the system. The most important step of the process of inspecting that product is the segmentation of the image into meaningful objects (defects and normal product). This paper presents an original approach along with other classical techniques for the segmentation of dual-band X-ray images of industrial products.*

Keywords: image segmentation, Hopfield neural networks, industrial quality inspection

1. INTRODUCTION

There are just a few products of industrial processes so well defined that their quality can be guaranteed to meet exactly the client specifications or requirements. However, in most areas of industrial processing some sort of testing or inspection has to be performed on intermediate or final products [1]. When dealing with small and simple batch products, it is easy and inexpensive to perform destructive testing on a sample of components, but in most of the industrial cases, non-destructive inspection techniques are employed.
Image segmentation is the first and the most important step in a contaminant/defect detection/inspection system used in the industry. Whereas such a system is used for detection of metallic or non-metallic contaminants (e.g. glass, bones and stones) or for detection of flaws or cracks), it usually involves some means of acquiring one or more images of the inspected product. The most important type of image used in commercial inspection systems is the X-ray image [1]-[5]. The detection of defects has to be reliable and cost efficient while performed with high speed [1]. Most segmentation methods currently rely on simple thresholding algorithms [7], [8], [9]. This paper concerns the use of a Competitive Hopfield Neural Network (CHNN) for the segmentation process of a dual-band image of industrial products.

2. EXPERIMENT

2.1. Classical approaches to x-ray images segmentation

A segmentation algorithm for an X-ray image needs to separate foreign objects (such as defects or contaminants) from the background (the normal product). One aims in separating not only entire objects from the background, but also separating only parts of objects from the background is also considered a successful technique. A simple thresholding of a the X-ray image would provide a useless result for further image analysis techniques. To illustrate this, an Otsu-based algorithm was implemented [8]. The product (an aluminum faucet obtained through casting – Fig. 1) contains three easily visible defects (Fig. 2 left).

A dual-band X-ray image [10] of the product has been acquisitioned (an image consisting of one high-energy and one low-energy X-ray images). Fig. 2 depicts the high-energy and low-energy X-ray images taken from the product. When thresholding the image, defects are merged with other parts of the background (normal product) and therefore, a correct extraction of important objects is not possible in this way, due to the fuzziness of the obtained X-ray dual-image. Therefore, multilevel thresholding techniques need to be employed to solve the segmentation problem.

Classical edge enhancement and detection techniques were also tested on the X-ray images. The aim here is to have a resultant image that contains contours for the foreign objects embedded in the product. The idea under lying edge detection is the computation of a local derivative operator. The first derivative of an edge modeled in this manner is 0 in all regions of constant grey level and constant during a grey-level transition. The first derivative of an image is called gradient. Results of applying classical edge detection techniques on a detail X-ray image (Fig. 3) are depicted in Fig. 4.

Classical methods of image segmentation applied to X-ray images with respect to an inspection system have proven to render results that are not very useful for further image analysis such as high-level detection (due to the merging between foreign-bodies and the surrounding background). Since image segmentation output is the input to consequent image processing techniques, one wants that output to be of a high quality. The segmentation process can also be seen as a constraint optimization problem. The constraints, in this case are based on the fact that objects extracted from the image needs to be homogenous and different from each other for instance. Thus, an alternative approach to image segmentation was implemented by using a Hopfield Neural Network architecture.

Fig. 1*. A part obtained through casting used for experiments*

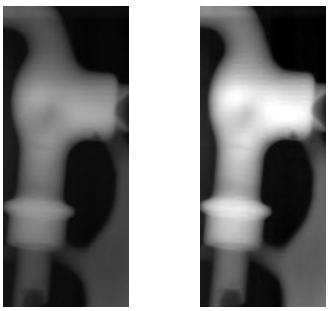

Fig. 2*. Dual band X-ray image of the faucet*

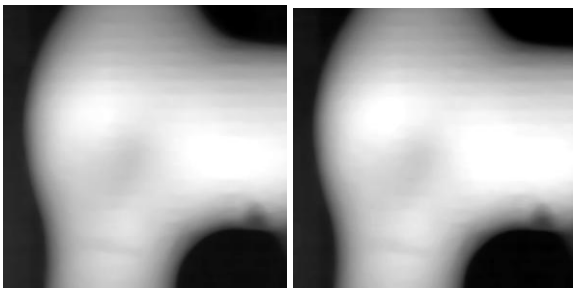

Fig.3. *X-ray detail of the faucet*

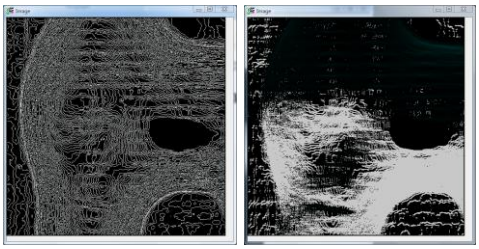

Fig. 4. *Classical Image segmentation algorithm results (Laplace – left, Gradient – right)*

2.2. Hopfield Neural Networks

Hopfield neural network (HNN) was proposed in 1985 by Hopfield as a way of solving optimization problems [11]. In a HNN each neuron is linked to another and weights are symmetrical, i.e. $w_{ij}=w_{ji}$, where w_{ij} represent the weight of connection between neuron *i* and *j*. There are no input or output neurons, but rather all the neurons look and act exactly the same. Inputs are applied to all neurons at the same time. The network for the optimization application tends to relax into stable states that minimizes an energy function of a Lyapunov form [11], [12], [13]:

$$E = -\sum_{i=1}^{N}\sum_{j=1}^{N} w_{ij} v_i v_j - \sum_{i=1}^{N} I_i v_i \tag{1}$$

where *N* is the number of neurons, v_i is the output of the i^{th} neuron , and I_i is the external input for the i^{th} neuron term. Hopfield demonstrated that HNN relax into a stable state tending to minimize its corresponding energy function. The behavior of the network in time can be determined by differentiating *E* with respect to v_i. The updating algorithm for a neuron *i*, at a given moment in time *t* is:

$$v_i^{[t]} = \sum w_{ij} v_j^{[t-1]} \tag{2}$$

The strategy used by the majority of the authors comprises two steps: firstly to find a binary representation for the segmentation solution, so that it can be mapped into a HNN stable state; and secondly, to define the energy function whose minimization will lead to an optimum solution to the problem. A Hopfield neural-network assigns each grey-level to a class according to a "goodness of segmentation" criteria. If a neuron *(i,j)* is active, then its corresponding grey-level *i* is assigned to class *j*. One grey-level can only be assigned to one class. The problem of segmenting an image of *n* by *n* pixels into *k* classes is to choose a suitable architecture for the HNN. In this study, we follow the ideas proposed in [14], [15], [16]. The solution of the segmentation process using a binary representation can be mapped using a grid of *P* rows of *k* neurons. The columns of this architecture represent the classes in which the image has to be segmented. The rows correspond to the objects that have to be assigned to a class according to some constraints. An approach taken by [7] is to use a grid of *P* by *k* neurons, where *P* is the total number of pixels in the image. Thus, the number of neurons in this approach is $n \times n \times k$. The computations associated with the behavior of such a neural network are very complex and unsuitable for a real time application. The complexity of such an approach can be decreased severely as in [16], [17]. Their HNN consists of a similar grid of *N* by *k* neurons, but in this case *N* is the number of grey-level values found in the input image (see Fig. 4). The number of neurons decreases dramatically to *Nxk*. This makes this architecture not only manageable from the point of view of computations involved, but also independent of the size of the image.

An energy function associated with a HNN must comprise terms for image segmentation constraints $E_{syntactic}$ or syntax energy i.e. to ensure that no grey-level or pixel can belong to two classes at the same time, and terms for goodness of segmentation, $E_{semantic}$ or the semantic energy:

$$E = E_{syntactic} + E_{semantic} \tag{3}$$

Using the binary mapping mentioned above, the segmentation constraints can be summarized as follows: only one neuron per row can be active (output is 1); this puts each grey-level into one class (left term of equation (4)); the sum of outputs of all neurons in one row is 1, this ensuring the fact that each grey-level belongs to only and only one class (right term of equation (4)):

$$E_{systactic} = \alpha \sum_{x=1}^{N} \left(\sum_{i=1}^{k} v_{xi} - 1 \right)^2 + \beta \sum_{x=1}^{N} \sum_{i=1}^{k} \sum_{\substack{j=1 \\ j \neq i}}^{k} v_{xi} v_{xj} \tag{4}$$

where α and β are constant values.

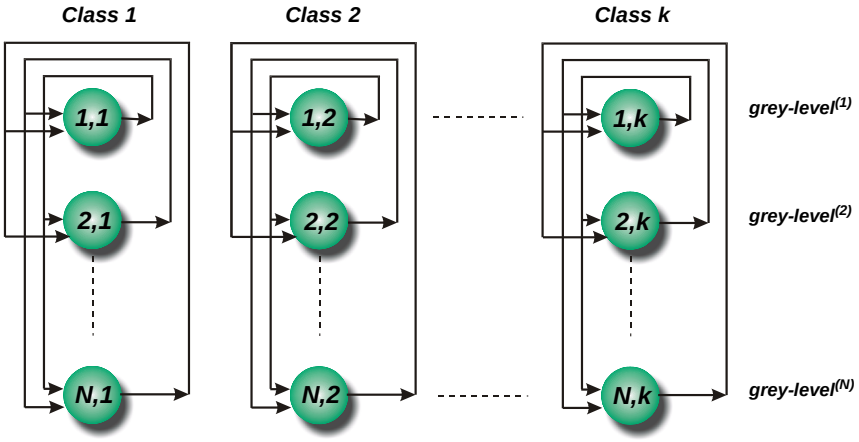

***Fig.4** HNN architecture*

The "goodness" of segmentation has to be measured by the following properties. Firstly, segments have to be uniform and homogenous with respect to grey-level values. Secondly, adjacent regions or segments have to have significant differences with respect to their uniformity (in this case the grey-level values). Thus, the semantic energy is defined in this case as the sum of square distances from each grey-level to the center of its class. By minimizing the energy, these distances decrease to a minimum leading to a solution for the segmentation. Due to the fact that two images are taken for each product, one high-energy X-ray and one low-energy X-ray image, a semantic energy for both images has to be defined as follows:

$$E_{semantic_1} = \vartheta \sum_{x=1}^{N_1} \sum_{y=1}^{N_1} \sum_{i=1}^{k} \frac{1}{\sum_{y=1}^{N} hl_y v_{yi}} v_{xi} DIS_{xy} hl_y v_{yi} + \delta \sum_{x=1}^{N_2} \sum_{y=1}^{N_2} \sum_{i=1}^{k} \frac{1}{\sum_{y=1}^{N} hh_y v_{yi}} v_{xi} DIS_{xy} hh_y v \tag{5}$$

where N_1 , N_2 are the number of grey-levels present in the low-energy respectively high-energy image, ϑ and δ are constants and hl_y and hh_y are the histogram values of the y grey-level for the low-energy band and high-energy band image respectively.

An important aspect in the process of defining the semantic energy is choosing the appropriate measure of distance DIS_{xy}. This represents the distance between grey-level l_x and grey-level l_y. Because the present method is actually a cluster analysis algorithm, a good segmentation can be defined by having spherical or ellipsoidal clusters. The squared Euclidian distance will allow hyperspherical distribution of clusters, formula that was used to determine DIS_{xy}:

$$DIS_{x,y} = d_{l_x,l_y} = (l_x - l_y)^2 \tag{6}$$

Using (4), (5) and (6) into (3) we derive the formula for the energy:

$$E = \alpha \sum_{x=1}^{N} \left(\sum_{i=1}^{k} v_{xi} - 1 \right)^2 + + \beta \sum_{x=1}^{N} \sum_{i=1}^{k} \sum_{\substack{j=1 \\ j \neq i}}^{k} V_{xi} V_{xj} + \eta \sum_{x=1}^{N} \sum_{y=1}^{N} \sum_{i=1}^{k} \frac{1}{\sum_{y=1}^{N} (hl_y + hh_y) v_{yi}} v_{xi} (l_x - l_y)^2 (hl_y + hh_y) v_{yi} \tag{7}$$

where $N = max(N_1, N_2)$.

A simplification of the energy equation can be done using a Winner Take All (WTA) scheme transforming HNN into a competitive architecture (CHNN). The input-output function for a neuron is modeled as to satisfy the constraints of the energy function. For every row, only one neuron can be active. The neuron that receives maximum input from all other neurons is declared winner and its output is set to 1; the output of the rest of neurons for the same row is set to zero:

$$V_{\substack{x,i \\ x=1..N \\ i=1..k}} = \begin{cases} 1, & \text{if } u_{x,i} = \max\left(v_{\substack{x,i \\ i=1..k}} \right) \\ 0, & \text{otherwise} \end{cases} \tag{8}$$

In other words, only one neuron is assigned 100% to a class. This satisfies the syntactic energy terms, therefore the energy equation (7) can be simplified to:

$$E = \sum_{x=1}^{N} \sum_{y=1}^{N} \sum_{i=1}^{k} \frac{1}{\sum_{y=1}^{N} (hl_y + hh_y) V_{yi}} V_{xi} DIS_{xy} (hl_y + hh_y) V_{yi} \tag{9}$$

Comparing equation (9) with the definition of the Lyapunov energy (1) one can compute the updating equation for the interconnection weights when no bias or threshold is present:

$$w_{\substack{(x,i)(y,j) \\ x,y=1..N \\ i,j=1..k}} = -\frac{1}{\sum_{y=1}^{N} (hl_y + hh_y) V_{yi}} V_{xi} DIS_{xy} (hl_y + hh_y) V_{yi} \tag{10}$$

where V_{xi} and V_{yi} are the binary values for the output of neurons *(x,i)* and *(y,i)*. Because the number of weights that needs to be updated is high, using the updating formula (2) and the weights updating formula (10), we have an equation for the total input to the neuron *(x,i)* :

$$v_{xi} = -\frac{1}{\sum_{y=1}^{N} (hl_y + hh_y) V_{yi}} \sum_{y=1}^{N} DIS_{xy} (hl_y + hh_y) V_{yi} \tag{11}$$

An algorithm was designed and implemented using the above equations. Segmentation into 3, 4 and 6 classes is depicted in Fig. 5 (for the image shown in Fig. 3).

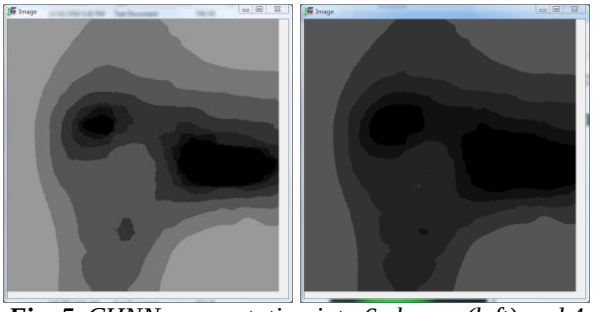

Fig. 5*. CHNN segmentation into 6 classes (left) and 4 classes (right)*

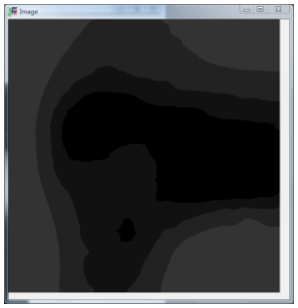

Fig. 6. CHNN *segmentation into 3 classes*

While classical algorithms may be able to detect some defects, CHNN successfully detects all defects, even though some of them only partially. Furthermore, during experimentation, it has been established that CHNN performs better on dual-band images than on single-band images, where some of the defects are missed. Since the number of classes must be specified *a priori*, further experimental work is necessary in order to find its optimum value. As it can be seen from Fig. 6, the segmentation into a large number of classes will lead to increased fragmentation of the segments, while the result of segmentation into only 3 classes (Fig. 6) is not satisfactory. The best results are obtained for 6 classes.

3. CONCLUSIONS

This paper concerns with using a Hopfield Neural Network in conjunction with a Winner Take All mechanism for segmentation of dual-band X-ray images. The number of computations associated with this algorithm is lower in comparison with other segmentation techniques proposed, i.e. morphological filtering [1]. The major advantage of this technique is the fact that only the histogram information of both images is used as opposed to spatial constraints that will lead to increased overhead. This study proved the applicability of CHNN for the detection of foreign bodies within a X-ray image. Future work will concentrate on minimizing even further the computational overhead involved and finding some means of post-processing the result.

Acknowledgments: The work has been co-funded by the Sectoral Operational Programme Human Resources Development 2007-2013 of the Romanian Ministry of Labour, Family and Social Protection through the Financial Agreement POSDRU/89/1.5/S/62557.

References

1. C.G. Amza, Intelligent X-ray Imaging Inspection System for the Food Industry, PhD Thesis, De Montfort University, Leicester, United Kingdom **(2002)**
2. *K.J. Burnham, Image segmentation, patent no. US2004/0258305 A1* ***(2004)***
3. *G.E. Georgeson, System, method and apparatus for the inspection of joints in a composite structure, patent no. US2003/0154801 A1* ***(2003)***
4. *E.J., Morton, et al., X-ray scanning system, patent no US7684538B2* ***(2010)***
5. *T. Moritake, et al., X-ray shielding device, patent no.US7500785 B2* ***(2009)***
6. *C.G. Amza, G. Tasca, Segmentation of Industrial X-ray images, Proceedings of the 4th WSEAS International Conference on Computational Intelligence CI'10, Bucharest, Romania, 2010, pp.54-59, ISSN: 1790-5117, ISBN 978-968-474-179-3* ***(2010)***
7. J.E. Koss, F.D. Newman, T.K. Johnson, D.L. Kirch, Abdominal organ segmentation using texture transforms and a Hopfield neural network, IEEE Transactions on Medical Imaging, **(1999)** vol.18, no.7, pp.640-648,

8. N. Otsu, A threshold selection method from grey-level histograms, IEEE Trans. On systems, man and Cybernetics, vol. SMC-9, no.1, pp.62-66, **(1979)**
9. N.R. Pal, S.K. Pal, A review on image segmentation techniques, Pattern Recognition, **(1993),** vol.26, no.9, pp.1277-1294
10. *C.G. Amza, Intelligent x-ray imaging inspection system for composite materials with polymeric matrix, Revista de materiale plastice, **(2007)** , nr.4, vol. 44(4), pp. 326-331*
11. J.J. Hopfield, Tank, D.W., "Neural" Computation of Decisions in Optimisation Problems, Biol.Cybern., **(1985)** vol.52, pp.141-152
12. J.J. Hopfield, Neural networks and physical systems with emergent collective computational abilities, Proc. Natl.Acad.Sci., USA, vol.79, pp.2554-2558, April **(1982)**
13. J.J. Hopfield, Neurons with graded response have collective computational properties like those of two-state neurons, Biophysics: Proc.Natl.Acad.Sci., USA, **(1984)** vol.81, pp.3088-3092
14. R. Poli, G. Valli, Hopfield neural networks for the optimum segmentation of medical images, Handbook of Neural Computation, Oxford University Press, chapter.G5.5, pp.1-10, **(1997)**
15. *D. Popescu, D. Anania, C.G. Amza, G. Amza, T. Cicic, Intelligent x-ray based training system for pedicle screw placement in lumbar vertebrae, Academic Journal of manufacturing Engineering, **(2011)** vol.9, Issue 1/2011, pp. 94-100, Ed. Politehnica, ISSN 1583-7904*
16. K.S. Cheng, J.S. Lin, C.W. Mao, The application of competitive Hopfield Neural Network to medical image segmentation, IEEE Transactions on Medical Imaging, vol.15, no.4, pp.560-567, August **(1996)**